

Unveiling Supersolid Order via Vortex Trajectory Correlations

Subrata Das* and Vito W. Scarola†

Department of Physics, Virginia Tech, Blacksburg, VA 24061, USA

The task of experimentally investigating the inherently dual properties of a supersolid, a simultaneous superfluid and solid, has become more critical following the recent experimental evidence for supersolids in dipolar Bose-Einstein condensates (BECs) of ^{164}Dy . We introduce a supersolid order parameter that uses vortex-vortex trajectory correlations to simultaneously reveal the periodic density of the underlying solid and superfluidity in a single measure. We propose experiments using existing technology to optically create and image trajectories of vortex dipoles in dipolar BECs. We numerically test our observable and find that vortex-vortex correlations reveal the supersolid lattice structure while distinguishing it from superfluidity. Our method sets the stage for experiments to use vortex trajectory correlations to investigate fundamental properties of supersolids arising from their dynamics and phase transitions.

The coexistence of a superfluid and solid at the same time and place defines a supersolid [1–4]. The superfluid component spontaneously breaks the $U(1)$ gauge symmetry of the many-body wavefunction with signatures such as quantized vortices and irrotational flow. Whereas the solid component spontaneously breaks translational symmetry with signatures that include persistent spatial oscillations in particle-particle correlations. Combined observation of such overlapping order parameters signals a supersolid, Fig. 1(a).

Definitive signatures of supersolids obtained from globally averaged observables are challenging to interpret. For example, torsional oscillation experiments were proposed to reveal irrotational flow of supersolid ^4He [5]. Experiments observing expected behavior [6] were brought into question [7, 8] by the prospect of solid dislocations and defects [4, 9] containing superfluid components that mimic irrotational flow expected in a supersolid.

The search for informative experimental probes of supersolids has become more pressing with the advent of engineered supersolidity [10] of ultracold bosonic atoms [11–27], particularly in highly magnetic atoms such as ^{164}Dy . The tunable dipole-dipole interaction between ^{164}Dy atoms allows strong interaction to drive the formation of periodic high-density crystalline structures (quantum droplets) [28–31] that spontaneously break translational invariance [27]. This solid gives way to a supersolid as the strength of dipolar interaction is lowered to become comparable to kinetic energy. Experiments identifying and probing dysprosium supersolids [15–26] rely on close support from theory [32–40].

Quantized vortices offer probes of superfluid order and therefore supersolids [41–46]. Several methods have been used to create vortices in atomic BECs. Rotation by stirring [47–49] was recently used to observe vortices in rotating supersolid ^{164}Dy [45]. Other methods include quenching [50–54], optical phase-engineering and holographic methods [55–58], and Laguerre-Gaussian (LG) beams [59–66]. Ref. 57 holographically created a vortex dipole (a pair of vortices with opposite angular momentum) [67] in a BEC with no net angular momentum thus

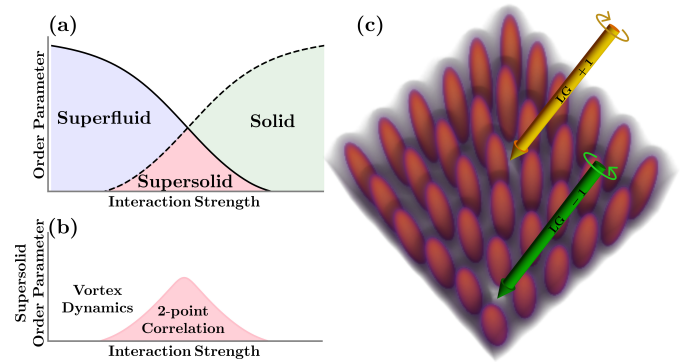


FIG. 1. (a) Schematic phase diagram where weak particle-particle interaction (compared to kinetic energy) favors a superfluid and strong interaction favors a solid. Overlapping order parameters define a supersolid. (b) The same as (a) but here a non-zero vortex-vortex trajectory correlation function offers a distinct supersolid order parameter. (c) Proposal to create a vortex dipole amid quantum droplets defining a quasi-two dimensional supersolid in a dipolar BEC using a pair of Laguerre-Gaussian beams.

avoiding net rotation. Furthermore, vortex dipoles move as quasiparticles making them excellent candidates for recent experimental advances observing vortex trajectories in BECs [68–73], including the use of non-destructive *in situ* trajectory imaging [74]. The creation of vortex dipoles and the direct imaging of their trajectories is therefore within reach of near-term experiments in supersolid ^{164}Dy .

We propose vortex-vortex correlations in trajectory imaging as quantitative probes of the fundamental duality inherent to supersolids, Fig. 1(b). Our central observation is that quantized vortices necessitate a superfluid component but also move along density gradient contours [75–77] to reveal the underlying lattice structure of a supersolid (akin to pair-correlations of the constituent bosons). Fig. 1(c) depicts a proposed experiment wherein a pair of LG beams creates vortex dipoles in a supersolid. We numerically test the efficacy of our setup

as a route to extract vortex-vortex trajectory correlations experimentally. We consider uniform [78] and harmonic traps. We find that our correlation function distinguishes the supersolid from the superfluid and, in the uniform trap, reveals the supersolid lattice structure.

Our proposal for a unique supersolid order parameter and its experimental implementation establishes a method for identifying supersolids, measuring lattice properties, tracking phase transitions, and monitoring supersolid lattice dynamics.

Model.— We consider N ^{164}Dy atoms trapped in an external potential $V_{\text{ext}}(\mathbf{r})$ while interacting via contact and dipolar interaction potentials [79–81]:

$$V_c(\mathbf{r}) = g\delta(\mathbf{r}) \quad \text{and} \quad V_{\text{dd}}(\mathbf{r}) = \frac{\mu_0\mu^2}{4\pi} \frac{1 - 3\cos^2\theta}{r^3}, \quad (1)$$

respectively. The contact interaction strength g is related to the s -wave scattering length a_s by $g = 4\pi\hbar^2 a_s/m$ where m is the mass of the atom, μ_0 is the vacuum permeability, and μ is the magnetic moment of the atom. The dipolar interaction strength varies with the angle θ between the relative position vector \mathbf{r} and the polarization direction (z -axis) of the dipole.

We model the dynamics of the entire system with the extended Gross-Pitaevskii equation (eGPE) [28, 82]:

$$i\hbar\frac{\partial}{\partial t}\psi(\mathbf{r}) = \left[-\frac{\hbar^2}{2m}\nabla^2 + V_{\text{ext}}(\mathbf{r}) + g|\psi(\mathbf{r})|^2 + \gamma|\psi(\mathbf{r})|^3 + \int d\mathbf{r}' V_{\text{dd}}(\mathbf{r} - \mathbf{r}')|\psi(\mathbf{r}')|^2 \right] \psi(\mathbf{r}). \quad (2)$$

Here, $\psi(\mathbf{r})$ is the system wavefunction normalized with $\int d\mathbf{r} |\psi|^2 = N$. The Lee-Huang-Yang [83–85] correction term contains $\gamma(\epsilon_{\text{dd}}) = (128\sqrt{\pi}\hbar^2 a_s^{5/2}/3m)(1 + \frac{3}{2}\epsilon_{\text{dd}}^2)$ [86, 87], which depends on the ratio of the dipolar length scale to a_s , $\epsilon_{\text{dd}} = a_{\text{dd}}/a_s$, where $a_{\text{dd}} = \mu_0\mu^2 m/(12\pi\hbar^2)$. ϵ_{dd} can be tuned using a Feshbach resonance in ^{164}Dy to vary a_s [27, 88] thus allowing exploration of phase transitions [82]. For ^{164}Dy , the dipole moment $\mu = 9.93\mu_B$, sets a dipolar length scale $a_{\text{dd}} = 131a_0$ where μ_B and a_0 are the Bohr magneton and Bohr radius, respectively. We choose $a_s = 94a_0$ ($\epsilon_{\text{dd}} = 1.39$) for and $110a_0$ ($\epsilon_{\text{dd}} = 1.19$) to achieve the supersolid and superfluid phases, respectively [16].

To study vortex dynamics in superfluid and supersolid phases, we assume two different external trapping potentials: (i) uniform in the xy plane and harmonic along z -axis, $V_{\text{ext}} = m\omega_z^2 z^2/2$ and (ii) an oblate 3D harmonic trap, $V_{\text{ext}} = m\omega^2(x^2 + y^2 + \lambda^2 z^2)/2$ where trapping anisotropy λ is the ratio of trapping frequency along the z -axis to that in the xy plane. In both cases, we induce vortex dipoles using the phase-imprinting method [89, 90] by multiplying the wavefunction $\psi(\mathbf{r})$ with a phase factor of $\exp[i\ell(y - y_0)/(x - x_0)]$. Here $\ell\hbar$, with $\ell = \pm 1$, is the vortex angular momentum and (x_0, y_0) is the vortex initial position.

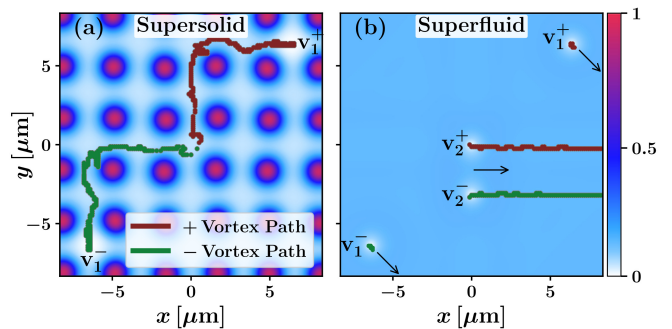


FIG. 2. Groundstate density profile in the $z = 0$ plane and vortex motion in a uniform trap in (a) supersolid and (b) superfluid phases. v_i^+ and v_i^- are the initial position of the $l = +1$ and $l = -1$ vortex of i -th vortex dipole. The red (green) line represents the trajectory of a $l = +1$ ($l = -1$) vortex. The black arrows in (b) represent the direction of motion of vortex dipoles in the superfluid phase. In (b), the simulations of vortex dipoles (v_1^+, v_1^-) and (v_2^+, v_2^-) are done separately and the background density is the product of two groundstates to identify the vortices.

Vortex motion in a uniform trap.— We first consider a uniform planar trap to ignore the effect of density variation due to trapping confinement. We solve the eGPE (2) using the split-step Crank-Nicolson method [91] and study the vortex dynamics in the system by tracking the vortex trajectories over time. In the uniform trap, $N = 1.3 \times 10^6$ atoms are trapped along the z -axis with $\omega_z = 2\pi \times 150$ Hz, and hard walls in the xy plane. The simulation box size is $L_x = L_y = 2L_z = 32.8\mu\text{m}$ and the grid size is $(256 \times 256 \times 128)$.

By solving the eGPE, we obtain the superfluid and supersolid ground state for different ϵ_{dd} . In a uniform trap the superfluid phase has a flat density profile whereas the supersolid phase shows a density modulation. The supersolid crystalline structure of quantum droplets contains a low density background, Fig. 1(c).

Vortices follow qualitatively distinct trajectories in the supersolid and superfluid phases. To see this, we dynamically imprint a vortex dipole. The vortex dipole will have a linear momentum in the superfluid phase which is inversely proportional to the separation d of $l = +1$ and $l = -1$ vortices [92, 93]. Both vortices therefore move in straight lines parallel to each other with a constant velocity in the superfluid. In contrast, in the supersolid phase, the vortex trajectories depend on non-uniform and periodic density patterns. In the vortex's frame of reference, density changes with time and space leading to a non-uniform force on the vortices. Due to this non-uniform force, vortices move in non-linear contours outlining the supersolid density gradient. In contrast to the superfluid phase, the vortex dipole is not stable in the supersolid phase and eventually annihilates when the $l = +1$ and $l = -1$ vortices approach each other. We test these qual-

itative expectations quantitatively using eGPE.

Figure 2 shows the vortex trajectories in the superfluid and supersolid phases. We choose a vortex dipole (v_1^+, v_1^-) in both phases as shown in Figs. 2(a) and 2(b). The $l = +1$ and $l = -1$ vortices follow non-uniform trajectories and eventually annihilate in the supersolid phase. While in the superfluid phase, they move in straight lines parallel to each other. The vortex dipole motion in the superfluid phase is stable, and they do not annihilate.

We verify that the velocity of the vortices is inversely proportional to the separation. In the superfluid phase we prepare a well separated $l = \pm 1$ vortex pair (v_1^+, v_1^-) . Fig. 2(b) shows that the distances traveled by this vortex dipole are small. In Fig. 2(b), we also show motion of a closely spaced vortex dipole (v_2^+, v_2^-) in the superfluid phase (this is studied separately from (v_1^+, v_1^-) , not shown in Fig. 2(a) for clarity of the figure). These vortices traveled a longer distance (full paths are not shown) compared to the vortex dipole (v_1^+, v_1^-) .

Correlation of vortex trajectories.— We now turn to our central proposal. Given distinct behavior of vortex motion in each phase we seek to extract quantitative information from the vortex trajectories. We define a vortex-vortex trajectory correlation function:

$$C(\mathbf{r}) = \langle s(\mathbf{r}_0)s(\mathbf{r}_0 + \mathbf{r}) \rangle, \quad (3)$$

where $s(\mathbf{r})$ is 1 if a vortex of any l passes through \mathbf{r} and 0 otherwise. In the following calculations we choose to compute $C(\mathbf{r})$ using trajectories of opposite l with no loss of generality. Note that $C(\mathbf{r})$ vanishes in the quantum droplet phase (because there is no phase coherence for vortices to form) and should show only trivial structure in the superfluid phase because the vortices move in straight lines. But in the supersolid phase, measurements of $C(\mathbf{r})$ will probe the underlying crystal structure of the supersolid. $C(\mathbf{r})$ can therefore be used as a supersolid order parameter. Importantly, the initial configuration of vortices must be chosen to break the underlying translational symmetry of the supersolid phase, otherwise straight-line trajectories will arise [94]. Straight trajectories will not allow measurements to distinguish between superfluid and supersolid states. In the following, we choose the initial positions of the vortex dipoles on the opposite arcs of a circle in the simulations to avoid biased choices in probing the quantum droplet square lattice in the supersolid phase.

We test the utility of $C(\mathbf{r})$ using eGPE simulations designed to replicate repeated measurements in a uniform trap. Figs. 3(a) and 3(b) show nine separate simulations of the resulting motion of the vortex dipoles $[(v_1^+, v_1^-), \dots, (v_9^+, v_9^-)]$ in both superfluid and supersolid phases. For all the vortex dipoles, the $l = +1$ and $l = -1$ vortex separation $d \approx 13\mu\text{m}$ is the same as shown by the initial position of the $l = +1$ ($l = -1$) vortex by red

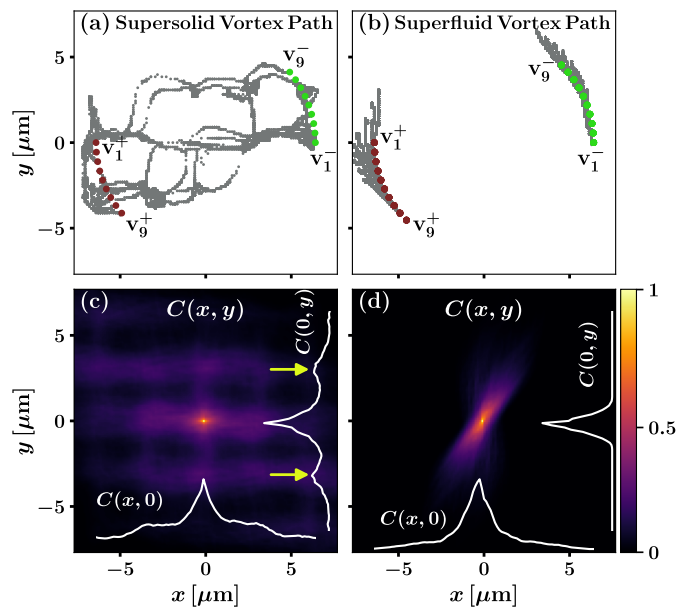


FIG. 3. Combined vortex trajectories of nine vortex dipoles $[(v_1^+, v_1^-), \dots, (v_9^+, v_9^-)]$ from separate simulations in (a) supersolid and (b) superfluid phases. The red (green) dots represent the initial position of the $l = +1$ ($l = -1$) vortex of the vortex dipoles. The grey lines represent the vortex trajectories. The correlation function $C(\mathbf{r})$ of the vortex trajectories in (c) superfluid and (d) supersolid phases. (c) and (d) show the correlation function $C(\mathbf{r})$ of the vortex trajectories in the supersolid and superfluid phases, respectively. In (c), apart from the primary peak at $\mathbf{r} = 0$, there are the secondary peaks at $\mathbf{r} \neq 0$ denoted by yellow arrows for $C(0, y)$. In contrast, in (d), the correlation function $C(\mathbf{r})$ shows only the primary peak at $\mathbf{r} = 0$. All simulation parameters are the same as in Fig. 2.

(green) dots in Figs. 3(a) and 3(b). We locate the vortex position at different instants of time and find the trajectories of the vortices as time evolves. We find different trajectories for different sets of initial positions of the vortices. By merging all of the trajectories we obtain a combined 2D trajectory on the xy plane shown in Figs. 3(a) and 3(b).

We find that even with a limited number of trajectories, $C(\mathbf{r})$ reveals aspects of the underlying lattice structure of the supersolid. Fig. 3(c) shows that the correlation function $C(\mathbf{r})$, apart from the primary trivial peak at $\mathbf{r} = 0$, shows secondary peaks at $\mathbf{r} \neq 0$ due to the non-uniform and periodic density patterns in the supersolid phase. Whereas in the superfluid phase, $C(\mathbf{r})$ shows only the primary peak at $\mathbf{r} = 0$ due to the straight-line motion of the vortices. Thus, the correlation function $C(\mathbf{r})$ of vortex trajectories is a useful tool to distinguish the superfluid and supersolid phases.

Use of $C(\mathbf{r})$ to probe a supersolid requires the following conditions to be met: (i) As mentioned above, initial positions must break the supersolid crystal symmetry. If initial vortex positions are chosen, for example, to be ran-

dom, a sufficient number of trajectories must be imaged to resolve auxiliary peaks. The limited number of runs in Fig. 3 were chosen near this threshold. (ii) Vortices are, ideally, to be used as non-invasive probes that leave the supersolid intact. We assume an LG beam spot size ($\sim 1\mu\text{m}$) below the supersolid lattice spacing ($\sim 3\mu\text{m}$ in our simulations) and with initial inter-vortex spacing high enough to avoid high vortex speeds. (iii) We assume the use of a uniform trap (or a sufficiently large number of atoms) to allow resolution of translational symmetry breaking. The supplementary material [94] shows data relaxing condition (i) in order to map the supersolid lattice whereas the following simulations relax conditions (ii) and (iii).

Vortex motion in a harmonic trap.— We now turn to small system sizes and harmonic trapping relevant for ongoing experiments. Tight trapping will limit the range of the solid and can even lead to spurious supersolid signatures [95]. We choose $N=80000$ atoms to be trapped in an oblate-shaped 3D harmonic trap with trapping frequencies $(\omega, \omega_z)=2\pi \times (45, 133)$ Hz [34], where ω is the transverse trapping frequency. The simulation box size is $L_x=L_y=L_z=30\mu\text{m}$.

We studied the motion of vortex dipoles in both superfluid ($a_s = 110a_0$) and supersolid ($a_s = 94a_0$) regimes. Without any vortices, the density profile of the superfluid is Gaussian, whereas the supersolid regime shows a single quantum droplet in the center of the trap with a low-density superfluid background [16, 18]. In both phases, we prepare ground states with a vortex dipole (v_1^+, v_1^-) separated by a distance $d \approx 6\mu\text{m}$, and we observe the motion of the vortices by tracking the vortex trajectories over time.

Figure 4(a) shows density profiles in the supersolid regime after the vortex dipole is imprinted. At $t = 0$ the creation of the vortices causes the single droplet at the center to split into multiple droplets. Over time, these droplets continuously deform and form at different locations due to the motion of the vortices. Here the dynamics explores a variety of metastable small supersolid configurations. Once the $l = \pm 1$ vortices annihilate each other, the small supersolid reaches an equilibrium state with three droplets, as we see at $t = 700$ ms in 4(a). The trajectories of the vortices are affected by the density modulation in the supersolid regime, moving in non-linear paths before annihilation [Fig. 4(b)]. In contrast, the vortices in the superfluid regime do not annihilate. They keep moving in an elliptical path with a constant speed, as shown in Fig. 4(c) [96, 97]. We therefore see that vortex dipole trajectories in the supersolid and superfluid regimes show qualitatively distinct behavior even in small systems with tight trapping.

Discussion.— We introduced and numerically tested a supersolid order parameter defined by correlations in vortex trajectories. Our tests used a limited number of trajectories to replicate sampling for near term experiments.

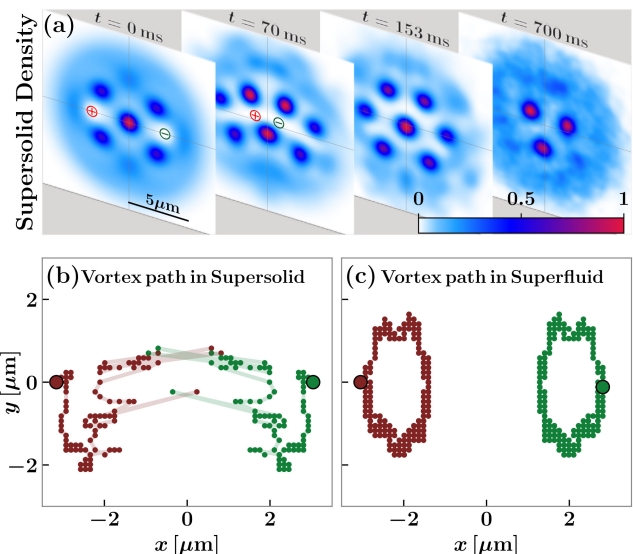


FIG. 4. (a) Snapshots of density profiles in the $z = 0$ plane at different times in the harmonic trap after the vortex dipole is imprinted in the supersolid phase. The red (green) circled “+” (“-”) marker represents the $l = +1$ ($l = -1$) vortex. (b) and (c) show the $l = +1$ (red dots) and $l = -1$ (green dots) vortex trajectories in the supersolid and superfluid regimes, respectively.

Larger numbers of samples allow resolution of complete supersolid lattice structures [94]. Our correlation function can also be used to study important properties of supersolids, including lattice dynamics due to supersolid phonons and phase transitions. Possible applications to different systems include exploration of broken translational symmetry in thin films of superfluid ^4He [98–100] and Fulde-Ferrell-Larkin-Ovchinnikov [101, 102] superconductors.

S.D. thanks Soumyadeep Halder and Bankim C. Das for the useful discussions. We acknowledge support from AFOSR-FA9550-23-1-0034, FA9550-19-1-0272 and ARO-W911NF2210247.

* subrata@vt.edu

† scarola@vt.edu

- [1] E. P. Gross, Unified Theory of Interacting Bosons, *Phys. Rev.* **106**, 161 (1957).
- [2] A. F. Andreev and I. M. Lifshitz, Quantum theory of defects in crystals, *Soviet Physics JETP* **29**, 1107 (1969).
- [3] G. V. Chester, Speculations on Bose-Einstein Condensation and Quantum Crystals, *Phys. Rev. A* **2**, 256 (1970).
- [4] M. Boninsegni and N. V. Prokof'ev, Colloquium: Supersolids: What and where are they?, *Rev. Mod. Phys.* **84**, 759 (2012).
- [5] A. J. Leggett, Can a Solid Be “Superfluid”?, *Phys. Rev. Lett.* **25**, 1543 (1970).
- [6] E. Kim and M. H. W. Chan, Probable observation of a

- supersolid helium phase, *Nature* **427**, 225 (2004).
- [7] D. Y. Kim and M. H. W. Chan, Absence of supersolidity in solid helium in porous vycor glass, *Phys. Rev. Lett.* **109**, 155301 (2012).
- [8] M. H. W. Chan, R. B. Hallock, and L. Reatto, Overview on solid 4He and the issue of supersolidity, *Journal of Low Temperature Physics* **172**, 317 (2013).
- [9] L. Pollet, M. Boninsegni, A. B. Kuklov, N. V. Prokof'ev, B. V. Svistunov, and M. Troyer, Superfluidity of grain boundaries in solid ^4He , *Phys. Rev. Lett.* **98**, 135301 (2007).
- [10] V. W. Scarola and S. Das Sarma, Quantum phases of the extended bose-hubbard hamiltonian: Possibility of a supersolid state of cold atoms in optical lattices, *Phys. Rev. Lett.* **95**, 033003 (2005).
- [11] M. Lu, N. Q. Burdick, S. H. Youn, and B. L. Lev, Strongly Dipolar Bose-Einstein Condensate of Dysprosium, *Phys. Rev. Lett.* **107**, 190401 (2011).
- [12] J. Léonard, A. Morales, P. Zupancic, T. Esslinger, and T. Donner, Supersolid formation in a quantum gas breaking a continuous translational symmetry, *Nature* **543**, 87 (2017).
- [13] J. Léonard, A. Morales, P. Zupancic, T. Donner, and T. Esslinger, Monitoring and manipulating Higgs and Goldstone modes in a supersolid quantum gas, *Science* **358**, 1415 (2017).
- [14] J.-R. Li, J. Lee, W. Huang, S. Burchesky, B. Shteynas, F. Ç. Top, A. O. Jamison, and W. Ketterle, A stripe phase with supersolid properties in spin-orbit-coupled Bose-Einstein condensates, *Nature* **543**, 91 (2017).
- [15] L. Tanzi, E. Lucioni, F. Famà, J. Catani, A. Fioretti, C. Gabbanini, R. N. Bisset, L. Santos, and G. Modugno, Observation of a Dipolar Quantum Gas with Metastable Supersolid Properties, *Phys. Rev. Lett.* **122**, 130405 (2019).
- [16] F. Böttcher, J.-N. Schmidt, M. Wenzel, J. Hertkorn, M. Guo, T. Langen, and T. Pfau, Transient Supersolid Properties in an Array of Dipolar Quantum Droplets, *Phys. Rev. X* **9**, 011051 (2019).
- [17] L. Tanzi, S. M. Rocuzzo, E. Lucioni, F. Famà, A. Fioretti, C. Gabbanini, G. Modugno, A. Recati, and S. Stringari, Supersolid symmetry breaking from compressional oscillations in a dipolar quantum gas, *Nature* **574**, 382 (2019).
- [18] L. Chomaz, D. Petter, P. Ilzhöfer, G. Natale, A. Trautmann, C. Politi, G. Durastante, R. M. W. van Bijnen, A. Patscheider, M. Sohmen, M. J. Mark, and F. Ferlaino, Long-Lived and Transient Supersolid Behaviors in Dipolar Quantum Gases, *Phys. Rev. X* **9**, 021012 (2019).
- [19] M. Guo, F. Böttcher, J. Hertkorn, J.-N. Schmidt, M. Wenzel, H. P. Büchler, T. Langen, and T. Pfau, The low-energy Goldstone mode in a trapped dipolar supersolid, *Nature* **574**, 386 (2019).
- [20] M. A. Norcia, C. Politi, L. Klaus, E. Poli, M. Sohmen, M. J. Mark, R. N. Bisset, L. Santos, and F. Ferlaino, Two-dimensional supersolidity in a dipolar quantum gas, *Nature* **596**, 357 (2021).
- [21] P. Ilzhöfer, M. Sohmen, G. Durastante, C. Politi, A. Trautmann, G. Natale, G. Morpurgo, T. Giamarchi, L. Chomaz, M. J. Mark, and F. Ferlaino, Phase coherence in out-of-equilibrium supersolid states of ultracold dipolar atoms, *Nat. Phys.* **17**, 356 (2021).
- [22] M. Sohmen, C. Politi, L. Klaus, L. Chomaz, M. J. Mark, M. A. Norcia, and F. Ferlaino, Birth, Life, and Death of a Dipolar Supersolid, *Phys. Rev. Lett.* **126**, 233401 (2021).
- [23] L. Tanzi, J. G. Maloberti, G. Biagioni, A. Fioretti, C. Gabbanini, and G. Modugno, Evidence of superfluidity in a dipolar supersolid from nonclassical rotational inertia, *Science* **371**, 1162 (2021).
- [24] M. A. Norcia, E. Poli, C. Politi, L. Klaus, T. Bland, M. J. Mark, L. Santos, R. N. Bisset, and F. Ferlaino, Can Angular Oscillations Probe Superfluidity in Dipolar Supersolids?, *Phys. Rev. Lett.* **129**, 040403 (2022).
- [25] T. Bland, E. Poli, C. Politi, L. Klaus, M. A. Norcia, F. Ferlaino, L. Santos, and R. N. Bisset, Two-Dimensional Supersolid Formation in Dipolar Condensates, *Phys. Rev. Lett.* **128**, 195302 (2022).
- [26] J. Sánchez-Baena, C. Politi, F. Maucher, F. Ferlaino, and T. Pohl, Heating a dipolar quantum fluid into a solid, *Nat Commun* **14**, 1868 (2023).
- [27] L. Chomaz, I. Ferrier-Barbut, F. Ferlaino, B. Laburthe-Tolra, B. L. Lev, and T. Pfau, Dipolar physics: A review of experiments with magnetic quantum gases, *Rep. Prog. Phys.* **86**, 026401 (2023).
- [28] F. Wächtler and L. Santos, Quantum filaments in dipolar Bose-Einstein condensates, *Phys. Rev. A* **93**, 061603 (2016).
- [29] F. Wächtler and L. Santos, Ground-state properties and elementary excitations of quantum droplets in dipolar Bose-Einstein condensates, *Phys. Rev. A* **94**, 043618 (2016).
- [30] D. Baillie and P. B. Blakie, Droplet Crystal Ground States of a Dipolar Bose Gas, *Physical Review Letters* **121**, 195301 (2018).
- [31] C. Mishra, L. Santos, and R. Nath, Self-Bound Doubly Dipolar Bose-Einstein Condensates, *Physical Review Letters* **124**, 073402 (2020).
- [32] S. M. Rocuzzo and F. Ancilotto, Supersolid behavior of a dipolar Bose-Einstein condensate confined in a tube, *Phys. Rev. A* **99**, 041601 (2019).
- [33] P. B. Blakie, D. Baillie, L. Chomaz, and F. Ferlaino, Supersolidity in an elongated dipolar condensate, *Phys. Rev. Res.* **2**, 043318 (2020).
- [34] S. Halder, K. Mukherjee, S. I. Mistakidis, S. Das, P. G. Kevrekidis, P. K. Panigrahi, S. Majumder, and H. R. Sadeghpour, Control of ^{164}Dy Bose-Einstein condensate phases and dynamics with dipolar anisotropy, *Phys. Rev. Res.* **4**, 043124 (2022).
- [35] S. Halder, S. Das, and S. Majumder, Two-dimensional miscible-immiscible supersolid and droplet crystal state in a homonuclear dipolar bosonic mixture, *Phys. Rev. A* **107**, 063303 (2023).
- [36] J. C. Smith, D. Baillie, and P. B. Blakie, Supersolidity and crystallization of a dipolar Bose gas in an infinite tube, *Phys. Rev. A* **107**, 033301 (2023).
- [37] B. T. E. Ripley, D. Baillie, and P. B. Blakie, Two-dimensional supersolidity in a planar dipolar Bose gas, *Phys. Rev. A* **108**, 053321 (2023).
- [38] K. Mukherjee, T. A. Cardinale, and S. M. Reimann, *Selective Rotation and Attractive Persistent Currents in Anti-Dipolar Ring Supersolids* (2024), arXiv:2402.19126 [cond-mat].
- [39] T. Bland, E. Poli, L. A. P. Ardila, L. Santos, F. Ferlaino, and R. N. Bisset, Alternating-domain supersolids in binary dipolar condensates, *Phys. Rev. A* **106**, 053322 (2022).
- [40] S. Halder, S. Das, and S. Majumder, Induced superso-

- lidity in a Dy-Er mixture, *Phys. Rev. A* **109**, 063321 (2024).
- [41] A. Gallemí, S. M. Roccuzzo, S. Stringari, and A. Recati, Quantized vortices in dipolar supersolid Bose-Einstein condensed gases, *Phys. Rev. A* **102**, 023322 (2020).
- [42] S. M. Roccuzzo, A. Gallemí, A. Recati, and S. Stringari, Rotating a Supersolid Dipolar Gas, *Phys. Rev. Lett.* **124**, 045702 (2020).
- [43] F. Ancilotto, M. Barranco, M. Pi, and L. Reatto, Vortex properties in the extended supersolid phase of dipolar Bose-Einstein condensates, *Phys. Rev. A* **103**, 033314 (2021).
- [44] T. Bland, G. Lamporesi, M. J. Mark, and F. Ferlaino, Vortices in dipolar Bose-Einstein condensates, *Comptes Rendus. Physique* **24**, 133 (2023).
- [45] E. Casotti, E. Poli, L. Klaus, A. Litvinov, C. Ulm, C. Politi, M. J. Mark, T. Bland, and F. Ferlaino, Observation of vortices in a dipolar supersolid (2024), [arXiv:2403.18510](https://arxiv.org/abs/2403.18510) [cond-mat, physics:quant-ph].
- [46] H. S. Ghosh, S. Halder, S. Das, and S. Majumder, Induced supersolidity and hypersonic flow of a dipolar Bose-Einstein Condensate in a rotating bubble trap (2024), [arXiv:2402.13422](https://arxiv.org/abs/2402.13422) [cond-mat].
- [47] K. W. Madison, F. Chevy, W. Wohlleben, and J. Dalibard, Vortex Formation in a Stirred Bose-Einstein Condensate, *Phys. Rev. Lett.* **84**, 806 (2000).
- [48] J. R. Abo-Shaeer, C. Raman, J. M. Vogels, and W. Ketterle, Observation of Vortex Lattices in Bose-Einstein Condensates, *Science* **292**, 476 (2001).
- [49] L. Klaus, T. Bland, E. Poli, C. Politi, G. Lamporesi, E. Casotti, R. N. Bisset, M. J. Mark, and F. Ferlaino, Observation of vortices and vortex stripes in a dipolar condensate, *Nat. Phys.* **18**, 1453 (2022).
- [50] L. E. Sadler, J. M. Higbie, S. R. Leslie, M. Vengalattore, and D. M. Stamper-Kurn, Spontaneous symmetry breaking in a quenched ferromagnetic spinor Bose-Einstein condensate, *Nature* **443**, 312 (2006).
- [51] C. N. Weiler, T. W. Neely, D. R. Scherer, A. S. Bradley, M. J. Davis, and B. P. Anderson, Spontaneous vortices in the formation of Bose-Einstein condensates, *Nature* **455**, 948 (2008).
- [52] G. Lamporesi, S. Donadello, S. Serafini, F. Dalfovo, and G. Ferrari, Spontaneous creation of Kibble-Zurek solitons in a Bose-Einstein condensate, *Nature Phys* **9**, 656 (2013).
- [53] S. Donadello, S. Serafini, T. Bienaimé, F. Dalfovo, G. Lamporesi, and G. Ferrari, Creation and counting of defects in a temperature-quenched Bose-Einstein condensate, *Phys. Rev. A* **94**, 023628 (2016).
- [54] J. Goo, Y. Lim, and Y. Shin, Defect Saturation in a Rapidly Quenched Bose Gas, *Phys. Rev. Lett.* **127**, 115701 (2021).
- [55] M. R. Matthews, B. P. Anderson, P. C. Haljan, D. S. Hall, C. E. Wieman, and E. A. Cornell, Vortices in a Bose-Einstein Condensate, *Phys. Rev. Lett.* **83**, 2498 (1999).
- [56] J. Denschlag, J. E. Simsarian, D. L. Feder, C. W. Clark, L. A. Collins, J. Cubizolles, L. Deng, E. W. Hagley, K. Helmerson, W. P. Reinhardt, S. L. Rolston, B. I. Schneider, and W. D. Phillips, Generating Solitons by Phase Engineering of a Bose-Einstein Condensate, *Science* **287**, 97 (2000).
- [57] J. F. S. Brachmann, W. S. Bakr, J. Gillen, A. Peng, and M. Greiner, Inducing vortices in a Bose-Einstein condensate using holographically produced light beams, *Opt. Express*, *OE* **19**, 12984 (2011).
- [58] A. Kumar, R. Dubessy, T. Badr, C. De Rossi, M. de Goër de Herve, L. Longchambon, and H. Perrin, Producing superfluid circulation states using phase imprinting, *Phys. Rev. A* **97**, 043615 (2018).
- [59] L. Allen, M. W. Beijersbergen, R. J. C. Spreeuw, and J. P. Woerdman, Orbital angular momentum of light and the transformation of Laguerre-Gaussian laser modes, *Physical Review A* **45**, 8185 (1992).
- [60] K.-P. Marzlin, W. Zhang, and E. M. Wright, Vortex Coupler for Atomic Bose-Einstein Condensates, *Phys. Rev. Lett.* **79**, 4728 (1997).
- [61] M. F. Andersen, C. Ryu, P. Cladé, V. Natarajan, A. Vaziri, K. Helmerson, and W. D. Phillips, Quantized Rotation of Atoms from Photons with Orbital Angular Momentum, *Physical Review Letters* **97**, 170406 (2006).
- [62] S. Beattie, S. Moulder, R. J. Fletcher, and Z. Hadzibabic, Persistent Currents in Spinor Condensates, *Phys. Rev. Lett.* **110**, 025301 (2013).
- [63] P. K. Mondal, B. Deb, and S. Majumder, Angular momentum transfer in interaction of Laguerre-Gaussian beams with atoms and molecules, *Phys. Rev. A* **89**, 063418 (2014).
- [64] A. Bhowmik, P. K. Mondal, S. Majumder, and B. Deb, Interaction of atom with nonparaxial Laguerre-Gaussian beam: Forming superposition of vortex states in Bose-Einstein condensates, *Phys. Rev. A* **93**, 063852 (2016).
- [65] S. Das, A. Bhowmik, K. Mukherjee, and S. Majumder, Transfer of orbital angular momentum superposition from asymmetric Laguerre-Gaussian beam to Bose-Einstein Condensate, *J. Phys. B: At. Mol. Opt. Phys.* **53**, 025302 (2020).
- [66] M. Ghosh Dastidar, S. Das, K. Mukherjee, and S. Majumder, Pattern formation and evidence of quantum turbulence in binary Bose-Einstein condensates interacting with a pair of Laguerre-Gaussian laser beams, *Physics Letters A* **421**, 127776 (2022).
- [67] T. W. Neely, E. C. Samson, A. S. Bradley, M. J. Davis, and B. P. Anderson, Observation of Vortex Dipoles in an Oblate Bose-Einstein Condensate, *Physical Review Letters* **104**, 160401 (2010).
- [68] P. C. Haljan, B. P. Anderson, I. Coddington, and E. A. Cornell, Use of Surface-Wave Spectroscopy to Characterize Tilt Modes of a Vortex in a Bose-Einstein Condensate, *Phys. Rev. Lett.* **86**, 2922 (2001).
- [69] B. P. Anderson, P. C. Haljan, C. E. Wieman, and E. A. Cornell, Vortex Precession in Bose-Einstein Condensates: Observations with Filled and Empty Cores, *Phys. Rev. Lett.* **85**, 2857 (2000).
- [70] P. Engels, I. Coddington, P. C. Haljan, and E. A. Cornell, Nonequilibrium Effects of Anisotropic Compression Applied to Vortex Lattices in Bose-Einstein Condensates, *Phys. Rev. Lett.* **89**, 100403 (2002).
- [71] D. V. Freilich, D. M. Bianchi, A. M. Kaufman, T. K. Langin, and D. S. Hall, Real-Time Dynamics of Single Vortex Lines and Vortex Dipoles in a Bose-Einstein Condensate, *Science* **329**, 1182 (2010).
- [72] S. Serafini, L. Galantucci, E. Iseni, T. Bienaimé, R. N. Bisset, C. F. Barenghi, F. Dalfovo, G. Lamporesi, and G. Ferrari, Vortex Reconnections and Rebounds in Trapped Atomic Bose-Einstein Condensates, *Phys. Rev. X* **7**, 021031 (2017).

- [73] S. W. Seo, B. Ko, J. H. Kim, and Y. Shin, Observation of vortex-antivortex pairing in decaying 2D turbulence of a superfluid gas, *Sci Rep* **7**, 4587 (2017).
- [74] K. E. Wilson, Z. L. Newman, J. D. Lowney, and B. P. Anderson, In situ imaging of vortices in Bose-Einstein condensates, *Phys. Rev. A* **91**, 023621 (2015).
- [75] P. Mason and N. G. Berloff, Motion of quantum vortices on inhomogeneous backgrounds, *Phys. Rev. A* **77**, 032107 (2008).
- [76] T. Simula, Vortex mass in a superfluid, *Phys. Rev. A* **97**, 023609 (2018).
- [77] A. J. Groszek, D. M. Paganin, K. Helmersson, and T. P. Simula, Motion of vortices in inhomogeneous Bose-Einstein condensates, *Phys. Rev. A* **97**, 023617 (2018).
- [78] A. L. Gaunt, T. F. Schmidutz, I. Gotlibovych, R. P. Smith, and Z. Hadzibabic, Bose-einstein condensation of atoms in a uniform potential, *Phys. Rev. Lett.* **110**, 200406 (2013).
- [79] C. J. Pethick and H. Smith, *Bose-Einstein Condensation in Dilute Gases*, 2nd ed. (Cambridge University Press, Cambridge, 2008).
- [80] L. Pitaevskii and S. Stringari, *Bose-Einstein Condensation and Superfluidity*, International Series of Monographs on Physics (Oxford University Press, Oxford, 2016).
- [81] T. Lahaye, C. Menotti, L. Santos, M. Lewenstein, and T. Pfau, The physics of dipolar bosonic quantum gases, *Rep. Prog. Phys.* **72**, 126401 (2009).
- [82] D. Baillie, R. M. Wilson, R. N. Bisset, and P. B. Blakie, Self-bound dipolar droplet: A localized matter wave in free space, *Phys. Rev. A* **94**, 021602 (2016).
- [83] T. D. Lee, K. Huang, and C. N. Yang, Eigenvalues and Eigenfunctions of a Bose System of Hard Spheres and Its Low-Temperature Properties, *Phys. Rev.* **106**, 1135 (1957).
- [84] A. R. P. Lima and A. Pelster, Quantum fluctuations in dipolar Bose gases, *Phys. Rev. A* **84**, 041604 (2011).
- [85] D. S. Petrov, Quantum Mechanical Stabilization of a Collapsing Bose-Bose Mixture, *Phys. Rev. Lett.* **115**, 155302 (2015).
- [86] R. Schützhold, M. Uhlmann, Y. Xu, and U. R. Fischer, Mean-field expansion in bose-einstein condensates with finite-range interactions, *Int. J. Mod. Phys. B* **20**, 3555 (2006).
- [87] A. R. P. Lima and A. Pelster, Beyond mean-field low-lying excitations of dipolar Bose gases, *Phys. Rev. A* **86**, 063609 (2012).
- [88] Y. Tang, W. Kao, K.-Y. Li, and B. L. Lev, Tuning the dipole-dipole interaction in a quantum gas with a rotating magnetic field, *Phys. Rev. Lett.* **120**, 230401 (2018).
- [89] A. E. Leanhardt, A. Görlitz, A. P. Chikkatur, D. Kielpinski, Y. Shin, D. E. Pritchard, and W. Ketterle, Imprinting Vortices in a Bose-Einstein Condensate using Topological Phases, *Phys. Rev. Lett.* **89**, 190403 (2002).
- [90] S. Bandyopadhyay, A. Roy, and D. Angom, Dynamics of phase separation in two-species Bose-Einstein condensates with vortices, *Physical Review A* **96**, 043603 (2017).
- [91] P. Muruganandam and S. Adhikari, Fortran programs for the time-dependent Gross-Pitaevskii equation in a fully anisotropic trap, *Computer Physics Communications* **180**, 1888 (2009).
- [92] K. Sasaki, N. Suzuki, and H. Saito, Bénard-von Kármán Vortex Street in a Bose-Einstein Condensate, *Phys. Rev. Lett.* **104**, 150404 (2010).
- [93] T. Aioi, T. Kadokura, T. Kishimoto, and H. Saito, Controlled Generation and Manipulation of Vortex Dipoles in a Bose-Einstein Condensate, *Phys. Rev. X* **1**, 021003 (2011).
- [94] See Supplemental Material.
- [95] V. W. Scarola, E. Demler, and S. Das Sarma, Searching for a supersolid in cold-atom optical lattices, *Phys. Rev. A* **73**, 051601 (2006).
- [96] W. Li, M. Haque, and S. Komineas, Vortex dipole in a trapped two-dimensional Bose-Einstein condensate, *Phys. Rev. A* **77**, 053610 (2008).
- [97] S. Middelkamp, P. J. Torres, P. G. Kevrekidis, D. J. Frantzeskakis, R. Carretero-González, P. Schmelcher, D. V. Freilich, and D. S. Hall, Guiding-center dynamics of vortex dipoles in Bose-Einstein condensates, *Phys. Rev. A* **84**, 011605 (2011).
- [98] S. Nakamura, K. Matsui, T. Matsui, and H. Fukuyama, Possible quantum liquid crystal phases of helium monolayers, *Phys. Rev. B* **94**, 180501 (2016).
- [99] J. Nyéki, A. Phillis, A. Ho, D. Lee, P. Coleman, J. Parpia, B. Cowan, and J. Saunders, Intertwined superfluid and density wave order in two-dimensional ^4He , *Nature Phys* **13**, 455 (2017).
- [100] J. Choi, A. A. Zadorozhko, J. Choi, and E. Kim, Spatially Modulated Superfluid State in Two-Dimensional He 4 Films, *Phys. Rev. Lett.* **127**, 135301 (2021).
- [101] P. Fulde and R. A. Ferrell, Superconductivity in a strong spin-exchange field, *Phys. Rev.* **135**, A550 (1964).
- [102] A. I. Larkin and Y. N. Ovchinnikov, Nonuniform state of superconductors, *Zh. Eksp. Teor. Fiz.* **47**, 1136 (1964), [*Sov.Phys.JETP* 20,762 (1965)].

Supplemental Material for “Unveiling Supersolid Order via Vortex Trajectory Correlations”

Subrata Das and Vito W. Scarola
 Department of Physics, Virginia Tech, Blacksburg, VA 24061, USA

I. SQUARE LATTICE VORTEX TRAJECTORY CORRELATION FUNCTIONS

In the main text we have shown the vortex trajectories for the vortex dipole where the $l = +1$ and $l = -1$ vortices are located on opposite arcs of a circle for the case of a uniform trap. Those trajectories break lattice symmetries and therefore will distinguish between the supersolid and superfluid regimes, whether there is a square or triangular lattice pattern in the supersolid. Furthermore, such symmetry breaking sampling of vortex trajectories will also yield the lattice spacing. Here, in the example of a square lattice supersolid, we assume prior knowledge of the lattice spacing and an approximate knowledge of the lattice structure. We demonstrate the ability of post-selection of the vortex trajectory correlations to yield more quantitative information on supersolid lattice structure.

The following simulations are performed to replicate a proposed experimental sampling protocol given lattice spacing and a square lattice hypothesis. We assume a large collection of data where initial vortex dipoles are imprinted to map out the lattice. Consider the set of data where vortices are imprinted near density maxima. For example, imagine a vortex dipole whose $l = +1$ vortex is located between 1 and 2 in Fig. S1(a), and the $l = -1$ vortex is located between 12 and 13. In that case, their trajectory will follow a *curved* path. We remove such curved trajectories from our data set.

We now consider trajectories to keep in the dataset. $l = +1$ and $l = -1$ vortices placed at density minima between droplets will move in nearly straight lines toward each other. In Fig. S1(a), if we choose the vortex dipole $(v^+, v^-) \equiv (1, 12)$, their trajectory is a nearly straight line connecting the $l = +1$ vortex (point 1) and $l = -1$ vortex (point 12). By post-selecting quasi-straight line trajectories we can obtain a vortex correlation function map of the supersolid lattice. Note that the vortex placement and post-selection process described here are biased and assume forehand knowledge of the lattice spacing and structure obtained from the method discussed in the main text.

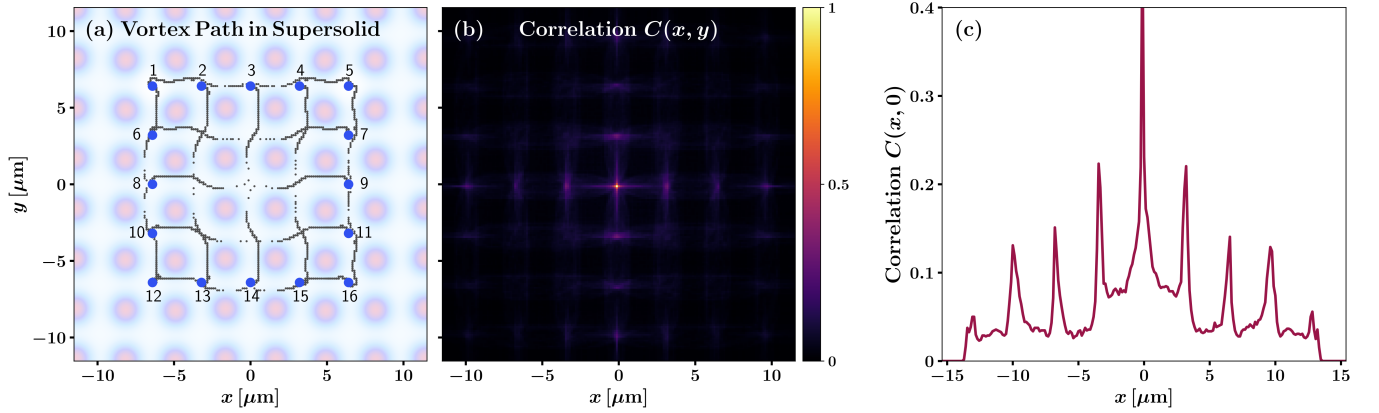


FIG. S1. Vortex trajectories and their correlations. (a) Vortex trajectories for different locations of the vortex dipole (v^+, v^-) from different simulations, where $(v^+, v^-) \equiv \{(1, 12), (2, 13), (3, 14), (4, 15), (5, 16), (1, 5), (6, 7), (8, 9), (10, 11), (12, 16)\}$ and the indices (1-16) correspond to the $l = +1$ or $l = -1$ vortex locations marked with blue marker. Trajectory of the vortex dipole (v^+, v^-) is an approximately straight line connecting v^+ and v^- . The opaque background shows the supersolid density of the ground state without vortices. Parameters, except for the initial vortex locations, are the same as Fig. 3a of the main text. (b) Vortex-vortex correlation function $C(x, y)$ calculated from different trajectories. (c) The correlation $C(x, 0)$ along x -axis.

Once quasi-straight line vortex trajectories have been post-selected, we can build the correlation function. We obtain the dynamics of the vortex dipole for different locations of the vortex dipole. All vortex dipoles are studied separately with the same parameters used in the main text for the uniform trap. Using these trajectories, we calculate the vortex-vortex correlation function $C(x, y)$ [Fig. S1(b)] and the correlation $C(x, 0)$ [Fig. S1(c)] along the x -axis. From the secondary peaks of the correlation function $C(x, 0)$, we can identify and find the periodicity of the square lattice structure.